

Action spectroscopy and temperature diagnostics of H_3^+ by chemical probing

J. Mikosch

Max-Planck-Institut für Kernphysik, Saupfercheckweg 1, 69117 Heidelberg, Germany
and Physikalisches Institut, Universität Freiburg, Hermann-Herder-Straße 3, 79104 Freiburg, Germany

H. Kreckel

Max-Planck-Institut für Kernphysik, Saupfercheckweg 1, 69117 Heidelberg, Germany

R. Wester^{a)}

Physikalisches Institut, Universität Freiburg, Hermann-Herder-Straße 3, 79104 Freiburg, Germany

R. Plašil and J. Glosík

Department of Electronics and Vacuum Physics, Charles University Prague, Mathematics and Physics Faculty, V Holešovičkách 2, Prague 8, Czech Republic

D. Gerlich

Institut für Physik, Technische Universität, 09107 Chemnitz, Germany

D. Schwalm and A. Wolf

Max-Planck-Institut für Kernphysik, Saupfercheckweg 1, 69117 Heidelberg, Germany

(Received 30 July 2004; accepted 7 September 2004)

Infrared absorption spectroscopy of few hundred H_3^+ ions trapped in a 22-pole ion trap is presented using chemical probing as a sensitive detection technique down to the single ion level. By exciting selected overtone transitions of the $(v_1=0, v_2=3^1) \leftarrow (0,0^0)$ vibrational band using an external cavity diode laser an accurate diagnostics measurement of the effective translational and rotational temperatures of the trapped ions was performed. The absolute accuracy of the measured transition frequencies was improved by a factor of four compared to previous plasma spectroscopy measurements using velocity modulation [Ventrudo *et al.*, *J. Chem. Phys.* **100**, 6263 (1994)]. The observed buffer gas cooling conditions in the ion trap indicate how to cool trapped H_3^+ ions into the lowest ortho and para rotational states. Future experiments will utilize such an internally cold ion ensemble for state-selected dissociative recombination experiments at the heavy ion storage ring Test Storage Ring (TSR). © 2004 American Institute of Physics. [DOI: 10.1063/1.1810512]

I. INTRODUCTION

The triatomic hydrogen molecular ion H_3^+ is one of the key molecules of interstellar chemistry; it is the main reaction agent in chemical networks responsible for the formation of more complex molecules in the interstellar medium. In fact, the effective formation reaction studied in detail by Glenewinkel-Mayer and Gerlich,¹



which is exothermic by 1.7 eV, renders H_3^+ the dominant ion in hydrogen plasmas at cold and moderate temperatures. Moreover, due to its fundamental importance as the most simple polyatomic molecule, H_3^+ is a much studied system both theoretically and experimentally.²

The recombination rate of H_3^+ with electrons constitutes a crucial parameters for modeling interstellar clouds³ and it is still a controversial issue. The last 40 years have seen numerous measurements of the thermal rate coefficient for dissociative recombination (DR) with electrons and the results have varied by several orders of magnitude.^{4,5} Different

rovibrational level populations have been discussed as one possible source of the discrepancies. Using the Coulomb explosion imaging technique at the Test Storage Ring (TSR) storage ring, it could be shown, however, that vibrationally excited states of H_3^+ relax within ~ 2 s of storage due to spontaneous radiative decay⁶ and have therefore no influence on DR measurements after long storage times. On the other hand, DR fragment imaging revealed the existence of long-lived rotational states with an effective temperature as high as 0.23 eV,⁷ which is in agreement with estimates from a rovibrational relaxation model⁶ based on transition strengths calculated by Tennyson and co-workers.⁸ Using a cold supersonic expansion ion source, a recent DR measurement with rotationally cold, albeit not state selected, H_3^+ ions was performed at the storage ring Cryring in Stockholm.⁹ It showed indeed a reduction in the derived DR rate coefficient for thermal electrons at 300 K by 40% to $6.8 \times 10^{-8} \text{ cm}^3 \text{ s}^{-1}$ compared to the best previous measurements at high rotational temperature.^{10,11} At the same time the discrepancy with stationary afterglow results that indicate a very low recombination rate of $< 4 \times 10^{-9} \text{ cm}^3 \text{ s}^{-1}$ is still unresolved.⁴

Theoretical calculations have for years not been able to yield H_3^+ DR rate coefficients that lie within an order of

^{a)}Author to whom correspondence may be addressed. Electronic mail: roland.wester@physik.uni-freiburg.de

magnitude of the measured rate coefficient, due to the involved multidimensional potential energy surfaces and the lack of a suitable curve crossing. However, in recent high-level nonadiabatic calculations of dissociative recombination through neutral Rydberg states coupled by Jahn-Teller interaction to the two ground state surfaces, a theoretical rate coefficient was obtained for the first time that is in reasonable agreement with the storage ring experiments.¹² In the same paper predictions for the rate coefficient of the two lowest ortho and para rotational states have been given, differing by a factor of 2 at 10 K; this could not be disentangled in the recent Crying experiment.

To investigate the dependence of the H_3^+ rate coefficient on the rotational state, with emphasis on the lowest para and ortho states, a new ion source based on a cryogenic ion trap was constructed¹³ for the storage ring TSR at the Max-Planck-Institut für Kernphysik in Heidelberg. In the 22 pole ion trap¹⁴ H_3^+ ions are trapped and sympathetically cooled in a buffer gas to temperatures of 10–100 K at which only the lowest rotational states are expected to be populated. Recently, it was demonstrated that about 4×10^5 ions can be stored in the ion trap and in experiments with HD and D_2 buffer gas the formation of deuterated clusters of up to 40 amu was observed, indicating the realization of temperatures well below room temperature.

Before embarking on H_3^+ DR measurements in the storage ring, we show in this work that rotational and translational degrees of freedom of the trapped H_3^+ ions indeed thermalize and under which conditions they may reach temperatures relevant for the interstellar medium.¹⁵ For this purpose we performed infrared action spectroscopy on the second vibrational overtone using a chemical reaction of vibrationally excited H_3^+ as the probing technique. The absence of a permanent dipole moment as well as stable electronically excited states render infrared spectroscopy the only feasible approach. Since the discovery of the first infrared lines in the laboratory in 1980,¹⁶ a number of spectroscopic studies of H_3^+ have been performed and more than 900 experimentally observed transitions are meanwhile documented (a comprehensive review can be found in Ref. 17).

Being of D_{3h} point group symmetry the vibrational modes of H_3^+ are characterized by the quantum numbers v_1 for the symmetric stretch and v_2^l for the doubly degenerate antisymmetric stretch vibration, the vibrational angular momentum l runs from $v_2, v_2 - 2, \dots, -v_2 + 2, -v_2$; only vibrational transitions that change the v_2 quantum number have non-negligible dipole matrix elements.¹⁷ Following Ref. 17 the rotational states of H_3^+ are labeled by their quantum numbers (J, G) (see Fig. 1). J is the total angular momentum associated with the motion of the nuclei. Instead of using the projection k of J onto the molecular symmetry axis, which is a good quantum number for most symmetric top molecules, one uses in H_3^+ the quantum number $G = |k - l|$, because of a near degeneracy for levels with the same G due to the Coriolis coupling to the vibrational angular momentum. For $l \neq 0$ and $(J - |l|) \geq G \geq 1$ there are two different ways to form the same G ; these two nondegenerate levels are labeled “ u ” for “upper” and “ l ” for “lower.” The Pauli principle, which

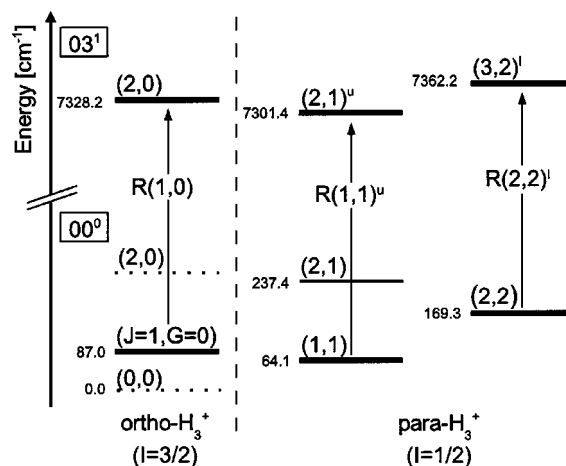


FIG. 1. Energy diagram of the lowest rotational states in the ground vibrational level of H_3^+ and the transitions (vertical arrows) to the rotational states of the $(0,3^+)$ vibrational level. The rotational states are labeled by their eigenenergy and their J and G quantum numbers following Ref. 17.

requires a totally antisymmetric wave function under nuclear permutations, links the total nuclear spin I , which is either $1/2$ for para- H_3^+ or $3/2$ for ortho- H_3^+ , to the G quantum number. $I = 3/2$ requires $G = 3n$ ($n = 0, 1, 2, \dots$) and $I = 1/2$ requires $G = 3n \pm 1$. In addition, certain $G = 0$ levels do not satisfy the symmetry requirements at all, most notably the $J = \text{even}$ levels in the ground vibrational state. For the R -branch ($\Delta J = +1$) transitions studied in this work the angular momentum selection rule is $\Delta G = 0$; these transitions are labeled by $R(J, G)^{u/l}$, where R denotes the R -branch, the (J, G) quantum numbers refer to the lower state and the superscript u/l reflects the corresponding u/l label of the upper state.¹⁷

Previous H_3^+ absorption studies measured direct absorption signals and thus required high H_3^+ number densities, long optical path lengths, and lock-in techniques such as velocity modulation due to the weak transition strengths of vibrational overtone transitions. Our approach relies on chemical probing of laser-excited states with more than two quanta of vibrations by the endothermic reaction



This is one of the few endothermic reactions of H_3^+ , which normally acts as a rapid proton donor in barrierless exothermic reactions. Detection of ArH^+ product ions is therefore a clear and very sensitive probe of vibrationally excited H_3^+ ions.

The earliest applications of chemical probing as a sensitive technique for action spectroscopy employed ion beams^{18,19} and ion flow tubes.²⁰ Recently, experiments in a multipole ion trap have employed chemical probing detection schemes to study electronic and vibrational spectroscopy of N_2^+ ²¹ and $C_2H_2^+$,^{22,23} respectively. Predissociation of weakly bound clusters after infrared excitation represents a similar action spectroscopy technique that has been used in a number of experiments (cf. Refs. 24 and 25).

In the experiment presented here we were able to use chemical probing spectroscopy to measure absorption profiles of the three lowest rotational transitions using only a

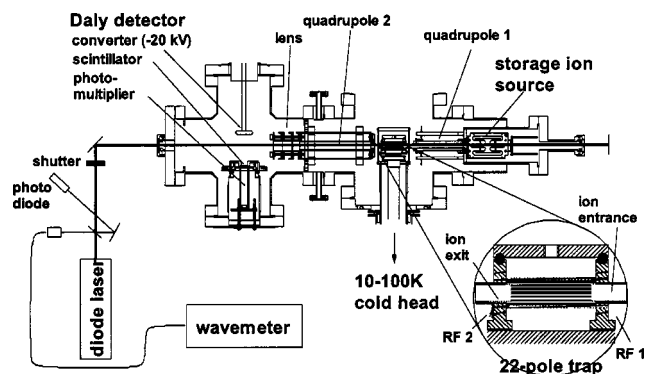


FIG. 2. Experimental setup including the storage ion source, the guiding quadrupole, the 22-pole ion trap and the product ion quadrupole mass spectrometer with the Daly detector. The laser light is passed axially through the trap and is retroreflected to increase the laser power. A commercial wavemeter yields an online measurement of the absolute laser frequency.

few hundred trapped H_3^+ ions (see Fig. 1). The experimental procedure will be outlined in the following section, followed by the presentation of results and a discussion of the thermalization process in the ion trap.

II. EXPERIMENTAL PROCEDURE

The major components of the experimental setup (see Fig. 2) are a storage ion source, an rf multipole ion trap and a product ion quadrupole mass spectrometer capable of single ion detection. High precision gas inlet valves allow to deliver hydrogen, helium, and argon gas (impurity fraction 10^{-4}) to the ion source and the ion trap. The infrared excitation light was delivered by a grating stabilized diode laser.

The H_3^+ ions were produced in a radiofrequency storage ion source.²⁶ Its main components are a stack of molybdenum plates with several U-shaped channels. The plates are electrically insulated by small ruby spheres between them and alternately connected to an rf signal of 12 MHz and 200 V amplitude peak to peak. During operation hydrogen gas is let into this structure by a sapphire precision valve and ionization is achieved by electron emission from a hot 0.3 mm rhenium filament situated above one side of the molybdenum stack. The H_2^+ ions created in collisions with the electrons are stored by the effective rf potential and thus they are likely to meet a neutral H_2 molecule in which case H_3^+ is produced. The ions are allowed to leave the volume only through a dedicated exit electrode that is connected to the entrance of the guiding quadrupole (quadrupole 1 in Fig. 2).

In the present experiment it was vital to keep the hydrogen pressure in the apparatus at a minimum in order to suppress the influence of H_2 on the buffer gas cooling as well as the destruction of ArH^+ formed in reaction (2) through the inverse reaction with H_2 molecules (see also Sec. III below). A differential pumping section between the ion source and the main chamber was not implemented, because the setup needs to be compact to be compatible with the ion accelerator of the storage ring TSR. The source was therefore operated at an estimated hydrogen pressure of about 10^{-4} mbar (resulting in a partial H_2 pressure of 4×10^{-7} mbar in the main vacuum chamber) at the expense of a comparatively

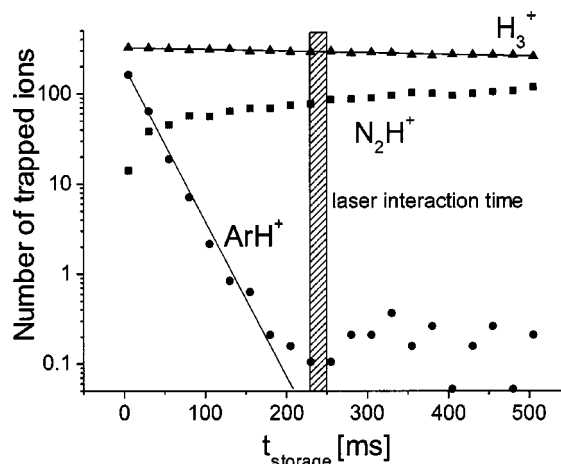


FIG. 3. Representative measurement of the number of stored ions as a function of the storage time in the 22-pole trap. H_3^+ , the dominant contribution, is found to decay slowly with a time constant longer than 2 s into N_2H^+ . About 25% of the H_3^+ ions carry initially enough vibrational energy to react immediately to ArH^+ , which then decays with a time constant of 25 ± 5 ms back to H_3^+ . During the laser interaction time (230–250 ms after injection) the number of H_3^+ ions in the trap amounts to 300 ± 20 while the initial ArH^+ fraction has decayed to a level below 1, small enough to allow the detection of laser-induced ArH^+ .

low H_3^+ ion yield. During operation as a source for the storage ring TSR a higher pressure and a correspondingly higher ion yield will be employed.

The 22-pole ion trap is the central part of the setup (see Fig. 2). Details of this trap have been published elsewhere²⁷ and only a brief description is given here. Storage is achieved by a cylindrical structure of 22 stainless steel rods planted alternately into two copper side plates that are supplied by an appropriate rf voltage (19.2 MHz, 30 V amplitude peak-to-peak). In this way a cylindrical effective potential is formed, similar to the classical Paul trap confinement but with the important difference that the potential walls are much steeper, since they scale with r .²⁰ In the axial direction the particles are trapped by small dc voltages (1–2 V) applied to cylindrical entrance and exit electrodes. The advantage compared to the traditional Paul trap arrangement is the large field free region in the center of the trap, which allows for a reduction of rf heating and thus permits improved thermalization of the ions' internal degrees of freedom.

The whole trap device is mounted on a cold head (Leybold Coolpower 2/10) capable of cooling the trap to a temperature of 10 K, measured with two silicon diode thermometers. For the current chemical probing spectroscopy experiment, the trap was heated to (55 ± 5) K using a heating filament at the base of the trap. The higher temperature was necessary to keep argon from freezing on the trap electrodes and to maintain an argon vapor pressure that is well above the argon partial pressure employed in the experiment.

The trap is loaded with a 10 μs long pulse of H_3^+ ions that is transported from the ion source into the trap through a quadrupole ion guide (quadrupole 1 in Fig. 2); the trap could be filled reproducibly over several days of operation with 300 ± 20 H_3^+ ions. Figure 3 shows a representative measurement of the number of trapped H_3^+ ions as a function of

TABLE I. Densities of the different gas constituents that are present inside the 22-pole ion trap during the experiment. Values are estimated to be accurate within a factor of 2.

| Gas constituent | Density in the trap (cm^{-3}) |
|-----------------|--|
| He | 4×10^{11} |
| Ar | 2×10^{11} |
| H_2 | 2×10^{10} |
| N_2 | $< 3 \times 10^8$ |

storage time. The lifetime of these ions in the trap is larger than 2 s and is limited by the proton transfer reactions with traces of N_2 molecules in the residual gas of the vacuum chamber, leading to the formation of N_2H^+ ions which are also trapped but which have no further influence on the experiment. The base pressure of the residual gas in the vacuum chamber amounts to about 8×10^{-9} mbar, corresponding to a particle density of $3 \times 10^8 \text{ cm}^{-3}$. With a large N_2 component in the residual gas this density explains well the measured H_3^+ decay constant, given that the proton transfer rate coefficient to N_2 amounts to about $2 \times 10^{-9} \text{ cm}^3/\text{s}$.

To achieve collisional cooling of the translational as well as internal degrees of freedom of the trapped H_3^+ ions the trap is flushed continuously with helium buffer gas. The gas density inside the trap is derived from a differential pressure measurement in the main vacuum chamber compared to the base pressure without buffer gas. The calibration factor linking the density inside the trap to the pressure reading in the main vacuum chamber follows from measuring a calibration reaction, in this case the decay of H_3^+ in reaction with D_2 . An independent calculation of the calibration factor relies on the conductance of the trap openings and the pumping speed connected to the chamber; it agrees with the calibration measurement well within the estimated accuracy of the density measurements of about a factor of 2.

In this experiment the employed helium density inside the trap was adjusted to about $4 \times 10^{11} \text{ cm}^{-3}$ (see Table I). Higher gas densities were not useful because the impurity concentration in the gas inlet system of 10^{-4} leads to a significantly faster H_3^+ decay in the trap. Through a second gas inlet argon is passed into the trap (particle density of about $2 \times 10^{11} \text{ cm}^{-3}$) to provide the neutral reactant for the chemical probing spectroscopy based on reaction (2) (see the following section). The typical collision time of trapped ions with the helium and argon buffer gas amounts to about 1–2 ms. The trapped H_3^+ ions were stored for 230 ms prior to the laser interaction (see Fig. 3). This allowed for about 100–200 buffer gas collisions, which is expected to be sufficient to achieve translational and rotational cooling. The time scale for vibrational cooling by buffer gas collisions is not known; however all vibrational levels decay by spontaneous radiative transitions,⁶ so that after 230 ms at most a small metastable fraction of the H_3^+ ions still populates the lowest symmetric stretch vibrations and are thus invisible to the absorption laser.

Both helium and argon are passed into the trap through teflon tubes wrapped around the cold head where they undergo a number of collisions with the tube walls which leads

to an efficient thermalization of the gas prior to entering the trap volume. The buffer gas atoms then stay inside the trap for about 100 collisions with the trap walls. Their translational temperature is therefore expected to be well characterized by the (55 ± 5) K trap wall temperature. An additional constituent of the buffer gas in the trap arises from an influx of H_2 molecules from the H_3^+ ion source, even at the low H_2 operating pressure in the ion source, due to the lack of a differential pumping stage. This influx leads to an H_2 density in the ion trap of about $2 \times 10^{10} \text{ cm}^{-3}$, obtained from the decay time of ArH^+ ions in the trap (see the following section).

To measure mass spectra of the stored ions after extraction from the trap a quadrupole mass spectrometer in combination with a Daly-type scintillation detector²⁸ is employed, which allows for the detection of single stored ions with nearly unity detection efficiency. The quadrupole consists of four stainless steel rods of 18 mm diameter (quadrupole 2 in Fig. 2) powered by an Extrel mass spectrometer power supply. The electrical arrangement allows for mass scans between 2 and 50 amu.

An infrared diode laser was used to deliver 1.38–1.39 μm radiation suitable for exciting H_3^+ into the (03^1) vibrational level. The employed laser was a commercial grid-stabilized diode laser system in Littmann–Metcalf^{29–31} configuration (Sacher). The linewidth of such lasers is typically below 10 MHz. Frequency scans over a range of 2 GHz were performed mode-hop free across the resonances using the piezoactuator on the end mirror of the external laser cavity. The absolute laser frequency was measured with an accuracy of ± 500 MHz using a commercial wavemeter (Burleigh). No active frequency locking was employed.

The optical setup is shown in Fig. 2. After having passed the apparatus the laser beam is retroreflected to increase the intensity in the interaction region. Continuous wavelength measurements with the wavemeter are achieved using a glass plate beamsplitter. A mechanical shutter³² allowed to pass the laser through the ion trap only during the desired storage times. This is monitored with the help of an InGaAs photodiode, onto which the backtraveling laser beam is focused. The laser power traversing the interaction region was estimated to be roughly 1.8 mW.

III. CHEMICAL PROBING SPECTROSCOPY

In the present experiment infrared absorption starting from several low lying rotational states of H_3^+ was measured indirectly using chemical probing based on reaction (2). This reaction is endothermic by 0.57 eV for H_3^+ in the vibrational ground state, i.e., it becomes only exothermic for molecules that have absorbed at least two quanta of vibrational energy. In particular, for excitations into the second overtone of the asymmetric stretch (03^1) it becomes exothermic by 0.23 eV. We expect that reactions of the vibrationally excited H_3^+ ions proceed with a large, Langevin limited rate coefficient of about $2 \times 10^{-9} \text{ cm}^3/\text{s}$, similar to most proton transfer reactions of ground state H_3^+ ions. At an argon buffer gas density in the trap of $2 \times 10^{11} \text{ cm}^{-3}$ this reaction should therefore proceed with a time constant of about 2 ms. This is faster

than the dominant competing decay process of H_3^+ in the $(0,3^1)$ level, namely radiative decay to lower vibrational levels, which is characterized by a 3 ms time constant.⁸ Mass spectrometric detection of the number of formed ArH^+ ions as a function of the laser frequency will therefore yield a direct action spectrum of the infrared absorption.

The fact that about 25% of the trapped H_3^+ ions are initially in high lying vibrational levels (due to inefficient cooling in the ion source given the low pressure conditions necessary for the absorption experiment) allowed us to observe the formation of ArH^+ ions according to reaction (2) without laser interaction during the first milliseconds of storage time. As viewed in Fig. 3 the ArH^+ ions undergo the inverse reaction with H_2 molecules back to H_3^+ and Ar with a lifetime of $\tau = 25 \pm 5$ ms. This lifetime yields the estimated H_2 density in the trap of $2 \times 10^{10} \text{ cm}^{-3}$, based on the rate coefficient for the inverse of reaction (2) of $2 \times 10^{-9} \text{ cm}^3/\text{s}$.³³ The ArH^+ decay has two important consequences for the experiment. On the one hand, the laser interaction time with the trapped H_3^+ ions was limited to 20 ms, because no further “breeding” occurs for longer storage times. On the other hand, the laser interaction has to occur at a storage time where the initial ArH^+ population has decayed to a level that is low enough to observe the laser-induced formation of ArH^+ ions. This was achieved for a laser interaction time of 230–250 ms of storage (see Fig. 3) where the ArH^+ level has decayed to an average level of well below one trapped ion. As described in the preceding section, this time window also leads to a good buffer gas cooling of the trapped H_3^+ ions while keeping the decay of H_3^+ to a minimum. Thus, in the experiment the trapped H_3^+ ions are buffer gas cooled for 230 ms and then irradiated by the infrared laser at given frequency for 20 ms. After that the ion trap is emptied and the ArH^+ product ions are counted after the quadrupole mass spectrometer. This cycle is repeated for each point of the laser frequency scan.

The formation rate $k_{(J,G)}(\nu_L)$ of ArH^+ per H_3^+ ion via an infrared transition $R(J,G)^{u/l}$ with transition frequency ν_0 is determined by the fraction $f_{(J,G)}(\nu - \nu_0)$ of the H_3^+ ions in the subensemble that can interact resonantly with the laser, the coupling strength of these ions to the laser field, given by the Einstein coefficient $B_{R(J,G)^{u/l}}$ and the spectral energy density of the laser $\rho(\nu - \nu_L)$ around its center frequency ν_L ,

$$k_{(J,G)}(\nu_L) = \int f_{(J,G)}(\nu - \nu_0) B_{R(J,G)^{u/l}} \rho(\nu - \nu_L) d\nu. \quad (3)$$

The fraction $f_{(J,G)}(\nu - \nu_0)$ depends on the relative population of the initial rotational state $p_{(J,G)}$, the geometrical overlap of the ion cloud with the laser beam, which is estimated from the ratio of the laser cross section to the trap cross section (A_L/A_{trap}) (about 10%), and due to the Doppler effect on the laser frequency ν . It is therefore given by

$$f_{(J,G)}(\nu - \nu_0) = p_{(J,G)} C e^{-(\nu - \nu_0)^2/2\sigma_D^2} \frac{A_L}{A_{\text{trap}}}, \quad (4)$$

where the normalization constant $C = \sqrt{mc^2/2\pi k_B T \nu_0^2}$, and the Doppler width is described by the standard deviation

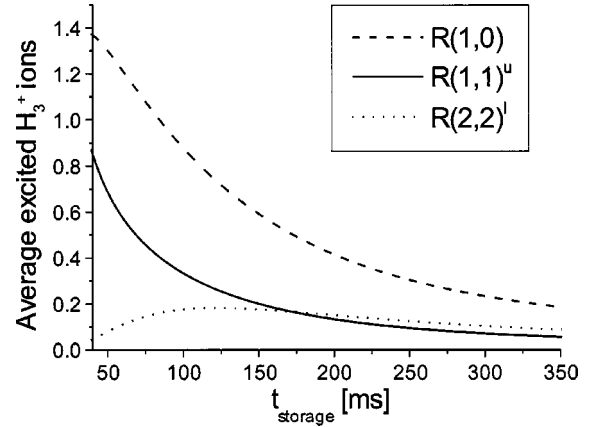


FIG. 4. Model calculation of the expected number of laser-excited H_3^+ ions as a function of temperature, assuming the rotational and translational temperature to be equal. Shown are results for the three infrared transitions studied in the experiment with the laser assumed to be on resonance. The expected average signal of less than one excited H_3^+ ion per trap filling required a low background and stable operating conditions.

$$\sigma_D = \sqrt{\frac{k_B T}{mc^2}} \nu_0. \quad (5)$$

T denotes the translational temperature of the ions. For our narrow bandwidth diode laser the spectral energy density $\rho(\nu - \nu_L)$ is approximated by a δ function times the energy density $P_L/A_L c$, where P_L is the laser power and c is the speed of light. Equation (3) then simplifies to

$$k_{(J,G)}(\nu_L) = \frac{P_{(J,G)} B_{R(J,G)^{u/l}} P_L}{A_{\text{trap}} c} C e^{-(\nu_L - \nu_0)^2/2\sigma_D^2}. \quad (6)$$

Note, that this rate is independent of the laser bandwidth, since at lower bandwidth less ions are addressed within the Doppler profile but with higher spectral intensity.

The total number of ArH^+ ions that are formed within the laser interaction time t_L is given by solving the rate equation

$$\frac{dN_{\text{ArH}^+}}{dt_L} = k_{(J,G)}(\nu_L) N_{\text{H}_3^+} - \frac{1}{\tau} N_{\text{ArH}^+}. \quad (7)$$

The first term accounts for the formation of ArH^+ from H_3^+ while the second term describes the backreaction of the ArH^+ ions with H_2 into H_3^+ with a time constant τ . As a result, one obtains

$$N_{\text{ArH}^+} = N_{\text{H}_3^+} k_{(J,G)}(\nu_L) \tau (1 - e^{-t_L/\tau}), \quad (8)$$

which is based on the safe assumption that depletion of the H_3^+ ions can be neglected during the laser interaction time.

Figure 4 shows a calculation of the number of expected ArH^+ ions, N_{ArH^+} , formed in the trap by resonant laser interaction as a function of the temperature T . The three curves display the result for the three lowest rotational states of H_3^+ . The calculation assumes a Boltzmann level population, calculated Einstein coefficients⁸ and a geometrical overlap of 10%. Furthermore, the number of trapped H_3^+ ions was assumed to be 250, corresponding to the situation in the experiment. Under these conditions we expect that the stron-

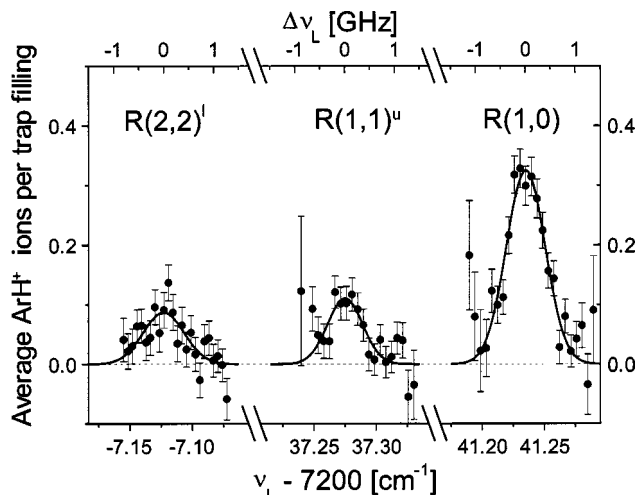


FIG. 5. Measured absorption profiles for the three observed transitions in the $(0,3^1)\leftarrow(0,0^0)$ vibrational overtone band. The employed chemical probing technique yields an ArH^+ ion per absorbed infrared photon. The signal is derived by averaging over 500 trap fillings, interleaved by 500 background measurements. The absolute accuracy of the frequency scale is $\pm 0.017 \text{ cm}^{-1}$.

gest signal is observed for the $R(1,0)(0,3^1)\leftarrow(0,0^0)$ transition over the whole temperature range from 40 K to 300 K. At 55 K we expect a signal strength of about 1.2 ArH^+ ions per trap filling when the laser is tuned into resonance. The $R(1,1)^u(0,3^1)\leftarrow(0,0^0)$ transition yields half of this signal estimate, about 0.6 ions per trap filling. The expected signal for the third transition $R(2,2)^l(0,3^1)\leftarrow(0,0^0)$ is lower by another factor of 5. Thus, the calculation shows that in order to observe absorption signals from the lowest rotational levels data has to be accumulated over many trap fillings. Stable conditions throughout continuous hours of measurement were therefore essential for this experiment.

IV. RESULTS

We have measured the absorption profiles of three infrared overtone transitions of H_3^+ via chemical probing spectroscopy which are displayed in Fig. 5. The spectra show the background-corrected number of detected ArH^+ ions per trap filling, plotted as a function of the laser detuning from the resonance. Approximately 500 trap fillings and background measurements, respectively, were averaged for each spectrum.

Based on Ref. 17 the three observed transitions are assigned to the $R(1,0)(0,3^1)\leftarrow(0,0^0)$, $R(1,1)^u(0,3^1)\leftarrow(0,0^0)$ and $R(2,2)^l(0,3^1)\leftarrow(0,0^0)$ transitions. Thus, the three observed transitions are R-branch transitions starting from the three energetically lowest rotational states of H_3^+ , which are located 64.1, 87.0, and 169.3 cm^{-1} above the symmetry forbidden virtual $|0,0\rangle$ ground state of H_3^+ (see the level scheme in Fig. 1). The most prominent signal is found for the transition starting in the $(1,0)$ state of the vibrational ground state.

Table II compares the center frequencies of the three observed peaks with the measurements and theoretical values presented in Refs. 34 and 17. The good agreement with the previous measurement within the experimental accuracy

TABLE II. Observed transitions in the $(0,3^1)\leftarrow(0,0^0)$ vibrational overtone band.

| Transition | $\nu_{\text{calc}} (\text{cm}^{-1})^a$ | $\nu_{\text{exp}} (\text{cm}^{-1})^b$ | $\nu_{\text{exp}} (\text{cm}^{-1})^c$ |
|------------|--|---------------------------------------|---------------------------------------|
| $R(1,0)$ | 7241.025 | 7241.244(70) | 7241.235(17) |
| $R(1,1)^u$ | 7237.058 | 7237.285(70) | 7237.277(17) |
| $R(2,2)^l$ | 7193.311 | 7192.908(70) | 7192.875(17) |

^aCalculated frequencies from Ref. 17.

^bMeasured frequencies from Ref. 34, accuracies are reassessed in Ref. 17.

^cThis work. Experimental accuracies are denoted in brackets.

proves our assignment of the three transitions, while a small, but significant discrepancy remains with respect to the calculated frequencies. As seen in Table II the accuracy of the present measurement is better by a factor of 4 as compared to the previous one. Note that the accuracy in our measurement is only limited by the absolute frequency uncertainty of the employed wavemeter.

The linewidths of the absorption profiles in Fig. 5 are dominated by Doppler broadening. Therefore the profiles unveil the translational velocities of the stored ions in the initial states of the transitions. Hence we can assign a translational temperature to the ions in these states. A Gaussian fit yielded a standard deviation of $\sigma_D = (470 \pm 30) \text{ MHz}$ for the strongest line and compatible values for the two weaker lines. According to Eq. (5) this corresponds to a translational temperature of $(170 \pm 20) \text{ K}$.

The relative population of each of the rotational states is obtained by dividing the amplitude of each resonance peak by the Einstein coefficient for the corresponding transition. We found that the populations of the three lowest rotational states correspond in energetically ascending order to 1:1.6(2):0.54(8). In thermal equilibrium the populations $P_{(J,G)}$ are linked to the temperature according to

$$\frac{P_{(J',G')}}{P_{(J,G)}} = \frac{g_{(J',G')}}{g_{(J,G)}} e^{-(E_{(J',G')} - E_{(J,G)})/(k_B T)}, \quad (9)$$

where the statistical weight $g_{(J,G)} = (2J+1)(2I+1)$ depends on the total rotational quantum number J as well as the total nuclear spin I . Using this equation the ratio of the measured populations of the two para states $(1,1)$ and $(2,2)$ is converted into an effective temperature which amounts to $(140 \pm 20) \text{ K}$. In the same way the population of the lowest para and the lowest ortho state can be used to derive an effective “para-to-ortho” rotational temperature of $(150 \pm 35) \text{ K}$, which has to be clearly distinguished from the translational and the “para” rotational temperatures because ortho-to-para conversion of H_3^+ can only occur in collisions with H_2 in this experiment.

V. DISCUSSION

In this paper we present the first infrared absorption measurements of cold, trapped H_3^+ ions using chemical probing as the detection technique. The high sensitivity of this approach is evident, given that each detected ArH^+ product ion reflects the absorption of a single infrared photon by a trapped H_3^+ ion. In the current experiment the excitation probability of an H_3^+ ion in the trap during the 20 ms of laser

irradiation amounts to about 0.1%, leading to the observed 0.1–0.3 ArH⁺ ions for 300 trapped H₃⁺ ions (see Fig. 5). This excitation probability is in reasonable agreement with our model calculation (see Fig. 4); the factor of 2 difference is most likely due to the uncertainty in the overlap of the laser beam with the trapped ions.

To enhance the sensitivity of the chemical probing spectroscopy technique, several improvements are envisioned. On the one hand, longer laser interaction times are possible if the lifetime of trapped ArH⁺ is extended by lowering the H₂ partial pressure, e.g., by differential pumping between the ion source and the trap. This would also allow for higher H₂ densities in the ion source and thus a larger yield of stored H₃⁺ ions. However, differential pumping is not implemented in the current trap setup, because it needs to be very compact to be compatible with the ion accelerator for the DR measurements in the storage ring TSR. On the other hand, stronger infrared laser sources can be employed, in particular when using a power build-up cavity to enhance the laser intensity inside the ion trap. Combining these aspects more than an order of magnitude increase in sensitivity seems feasible. An extension of the technique to lower trap temperatures is possible if the argon gas is not thermalized with the trap walls, which would lead to freeze-out, but is instead passed through the trap, e.g., as a pulsed supersonic beam. An alternative, promising approach to measure state populations at very low temperatures is to study the change in the reaction equilibrium of deuteration reactions in the presence of the absorption laser.

In this work, three different effective temperatures are derived from the absorption profiles of the three observed transitions, the translational “Doppler” temperature of the ions (170±20 K) and two effective rotational temperatures associated with the relative population of two para-states (140±20 K) and with the relative population of the lowest ortho state to the lowest para state (150±35 K). All three effective H₃⁺ temperatures are consistent with each other within the experimental accuracy. This may not necessarily be the case, because the translational and the rotational temperature of the separate ortho and para systems thermalize in collisions with the dominant buffer gases helium and argon, whereas ortho-to-para conversion may only occur in collisions with normal H₂ by nuclear spin re-arrangement in the H₅⁺ collision complex. Thus the ortho-to-para temperature is not a priori expected to reflect the translational or rotational temperature.

The translational and internal temperature of the trapped H₃⁺ ions of about 150 K is significantly larger than the 55 K temperature of the rf trap and the helium buffer gas. Three different mechanisms may explain this deviation. On the one hand, electric field inhomogeneities near the trap electrodes may lead to large amplitudes of the rf micromotion in the trap which may convert rf energy into translational and subsequently internal energy. Impurities on the rf electrodes of the trap, e.g., due to the freeze-out of argon, may introduce such patch fields. While high-order multipole rf traps have in general the property to minimize this effect, its contribution to the H₃⁺ temperature cannot be ruled out in the present experiment. On the other hand, the background gas in the

vacuum chamber that penetrates into the ion trap, predominantly H₂ from the ion source (see Table I), may not thermalize quickly enough with the trap walls, and thus leads to collisional heating of the trapped ions. However, this effect may not explain a temperature increase by more than about 10 K, because the helium and argon densities together are larger than the H₂ density by a factor of 30 and both the helium and argon buffer gas are carefully thermalized to the 55 K of the cold head, before the gas enters the ion trap. Nevertheless, the approximately 10 H₂ collisions that an H₃⁺ ion undergoes inside the trap may be enough to equilibrate the ortho-to-para temperature through an intermediate H₅⁺ collision complex. The third heating mechanism originates from the normal mixture of the ortho and para states of the H₂ gas component in the ion trap. Thus, 75% of the H₂ molecules are expected to occupy the lowest ortho state with $J=1$, which carries a rotational energy of about $120\text{ cm}^{-1} = k_B \times 180\text{ K}$. Quenching of the excited ortho-H₂ states in collisions with the trap walls only occurs with lifetimes of days. It is therefore possible that this energy is converted in collisions with the stored ions into H₃⁺ internal or translational excitation. At present, it is not clear, which of these heating mechanisms plays the dominant role for the increase of the translational and rotational temperature of the stored H₃⁺ ions with respect to the helium and argon buffer gas.

The ion trap is designed to produce rotationally cold H₃⁺ ions for dissociative recombination experiments at the storage ring. For this purpose it will be operated at 10 K instead of 55 K. At these temperatures impurities play practically no role, because all gas impurities freeze out and only hydrogen and helium remain gaseous inside the trap. Much higher buffer gas densities can therefore be employed without affecting the H₃⁺ lifetime. If the helium buffer gas density is a factor of 1000 higher than in the present experiment, all of the above discussed heating mechanisms are expected to play a much smaller role and the ion temperature may well fall below 15 K for 10 K buffer gas temperature. At these temperatures only the lowest para and the lowest ortho states of H₃⁺ are expected to be populated. The relative population of these two states depends predominantly on the efficiency of ortho-to-para conversion and not on the translational temperature of the buffer gas. To prepare all H₃⁺ ions in a single quantum state, namely the lowest para-state, it will be necessary to add also para-H₂ buffer gas.

VI. CONCLUSIONS

In this paper we present results on chemical probing infrared absorption spectroscopy of a few hundred trapped H₃⁺ ions. One of the few endothermic ion-molecule reactions of H₃⁺, the proton transfer reaction with argon, was utilized to detect the absorption of an infrared photon. Specifically, the ArH⁺ product ions were detected that were formed in reactive collisions of vibrationally excited H₃⁺ ions with argon, before radiative decay can occur.

Three rovibrational transitions of the (0,3¹)←(0,0⁰) band were observed, the $R(1,0)$, $R(1,1)^u$, and $R(2,2)^l$ transitions. The measured transition frequencies agree well with the previous values,³⁴ but the accuracy of the transition fre-

quencies could be increased by a factor of four relative to the previous measurement and was only limited by the accuracy of the employed wavemeter. This demonstrates that chemical probing spectroscopy with trapped ions is indeed capable of producing high-resolution spectra with a very high sensitivity.

From the Doppler profiles and the amplitudes of the three absorption peaks the effective translational and internal temperatures of the trapped H_3^+ ions were derived. They agree well with an overall temperature of 150 ± 20 K. This ion temperature, which is about three times larger than the helium buffer gas temperature, may be explained by heating due to rf micromotion or by heating due to the H_2 constituent of the buffer gas, in particular energy transfer from ortho- H_2 .

In the near future the H_3^+ ions from the trap will be employed in rotational-state-selected dissociative recombination experiments at the Heidelberg storage ring TSR. In these experiments the trap will be operated at 10 K where only lowest ortho and para rotational states of H_3^+ will be populated.

ACKNOWLEDGMENTS

We wish to acknowledge support by A. Hillenbach in setting up the rf ion trap. We also thank M. Weidemüller for many fruitful discussions. J.G. acknowledges financial support by GACR (Grant No. 205/02/0610). This work was supported by the EU research training network "electron transfer reactions" under Contract No. HPRN-CT-2000-0142.

¹T. Glenewinkel-Meyer and D. Gerlich, *Isr. J. Chem.* **37**, 343 (1997).

²J. Tennyson, *Rep. Prog. Phys.* **57**, 421 (1995).

³G. P. de Forets and E. Roueff, *Philos. Trans. R. Soc. London, Ser. A* **358**, 2433 (2000).

⁴R. Plašil, J. Glosik, V. Poterya, P. Kudrna, J. Ruzs, M. Tichý, and A. Pysanenko, *Int. J. Mass. Spectrom.* **218**, 105 (2002).

⁵M. Larsson, *Philos. Trans. R. Soc. London, Ser. A* **358**, 2433 (2000).

⁶H. Kreckel, S. Krohn, L. Lammich *et al.*, *Phys. Rev. A* **66**, 052509 (2002).

⁷D. Strasser, L. Lammich, S. Krohn *et al.*, *Phys. Rev. Lett.* **86**, 779 (2001).

⁸L. Neale, S. Miller, and J. Tennyson, *Astrophys. J.* **464**, 516 (1996).

⁹B. J. McCall, A. J. Huneycutt, R. J. Saykally *et al.*, *Nature (London)* **422**, 500 (2003).

¹⁰G. Sundström, J. R. Mowat, H. Danared *et al.*, *Science* **263**, 785 (1994).

¹¹M. J. Jensen, H. B. Pedersen, C. P. Safvan, K. Seiersen, X. Urbain, and L. H. Andersen, *Phys. Rev. A* **63**, 052701 (2001).

¹²V. Kokoouline and C. H. Greene, *Phys. Rev. Lett.* **90**, 133201 (2003).

¹³H. Kreckel, Ph.D. thesis, Universität Heidelberg, 2003.

¹⁴D. Gerlich, *Adv. Chem. Phys.* **82**, 1 (1992).

¹⁵D. Gerlich, E. Herbst, and E. Roueff, *Planet. Space Sci.* **50**, 1275 (2002).

¹⁶T. Oka, *Phys. Rev. Lett.* **45**, 531 (1980).

¹⁷C. M. Lindsay and B. J. McCall, *J. Mol. Spectrosc.* **210**, 60 (2001).

¹⁸A. Carrington, D. R. J. Milverton, and P. J. Sarre, *Mol. Phys.* **35**, 1505 (1978).

¹⁹W. H. Wing, G. A. Ruff, J. W. E. Lamb, and J. J. Spezeski, *Phys. Rev. Lett.* **36**, 1488 (1976).

²⁰F. J. Grieman, J. C. Hansen, and J. T. Moseley, *Chin. Phys. Lett.* **85**, 53 (1982).

²¹S. Schlemmer, T. Kuhn, E. Lescop, and D. Gerlich, *Int. J. Mass. Spectrom.* **185/186/187**, 589 (1999).

²²S. Schlemmer, E. Lescop, J. von Richthofen, D. Gerlich, and M. Smith, *J. Chem. Phys.* **117**, 2068 (2002).

²³O. Asvany, T. Giesen, B. Redlich, and S. Schlemmer (unpublished).

²⁴K. R. Asmis, N. L. Pivonka, G. Santambrogio, M. Brümmer, C. Kaposta, D. M. Neumark, and L. Wöste, *Science* **299**, 1375 (2003).

²⁵J.-W. Shin, N. I. Hammer, E. G. Diken, M. A. Johnson, R. S. Walters, T. D. Jaeger, M. A. Duncan, R. A. Christie, and K. D. Jordan, *Science* **304**, 1137 (2004).

²⁶E. Telay and D. Gerlich, *Chem. Phys.* **4**, 417 (1974).

²⁷D. Gerlich, *Phys. Scr.*, **T59**, 256 (1995).

²⁸N. R. Daly, *Rev. Sci. Instrum.* **31**, 264 (1960).

²⁹M. G. Littman, *Opt. Lett.* **3**, 138 (1978).

³⁰K. Liu and M. G. Littman, *Opt. Lett.* **6**, 117 (1980).

³¹P. McNicholl and H. J. Metcalf, *Appl. Opt.* **24**, 2757 (1985).

³²K. Singer, S. Jochim, M. Mudrich, A. Mosk, and M. Weidemüller, *Rev. Sci. Instrum.* **73**, 4402 (2002).

³³D. K. Bedford and D. Smith, *Int. J. Mass. Spectrom.* **98**, 179 (1990).

³⁴B. F. Ventrudo, D. T. Cassidy, Z. Y. Guo, S. Joo, S. S. Lee, and T. Oka, *J. Chem. Phys.* **100**, 6263 (1994).